

## Research Article

# Microstructure and Nonohmic Properties of $\text{SnO}_2\text{-Ta}_2\text{O}_5\text{-ZnO}$ System Doped with $\text{ZrO}_2$

Xiuli Fu,<sup>1</sup> Feng Jiang,<sup>2</sup> Ruichao Gao,<sup>1,2</sup> and Zhijian Peng<sup>2</sup>

<sup>1</sup> School of Science, Beijing University of Posts and Telecommunications, Beijing 100876, China

<sup>2</sup> School of Engineering and Technology, China University of Geosciences, Beijing 100083, China

Correspondence should be addressed to Xiuli Fu; [xiulifu@bupt.edu.cn](mailto:xiulifu@bupt.edu.cn) and Zhijian Peng; [pengzhijian@cugb.edu.cn](mailto:pengzhijian@cugb.edu.cn)

Received 7 August 2013; Accepted 26 November 2013; Published 20 January 2014

Academic Editors: M. J. Hua, R. Parra, and K. Prabhakaran

Copyright © 2014 Xiuli Fu et al. This is an open access article distributed under the Creative Commons Attribution License, which permits unrestricted use, distribution, and reproduction in any medium, provided the original work is properly cited.

The microstructure and nonohmic properties of  $\text{SnO}_2\text{-Ta}_2\text{O}_5\text{-ZnO}$  varistor system doped with different amounts of  $\text{ZrO}_2$  (0–2.0 mol%) were investigated. The proposed samples were sintered at 1400°C for 2 h with conventional ceramic processing method. By X-ray diffraction,  $\text{SnO}_2$  cassiterite phase was found in all the samples, and no extra phases were identified in the detection limit. The doping of  $\text{ZrO}_2$  would degrade the densification of the varistor ceramics but inhibit the growth of  $\text{SnO}_2$  grains. In the designed range, varistors with 1.0 mol%  $\text{ZrO}_2$  presented the maximum nonlinear exponent of 15.9 and lowest leakage current of 110  $\mu\text{A}/\text{cm}^2$ , but the varistor voltage increased monotonously with the doping amount of  $\text{ZrO}_2$ .

## 1. Introduction

$\text{SnO}_2$  varistors are semiconducting ceramic devices, which possess nonlinear voltage-current characteristics due to their grain boundary effects formed commonly by sintering  $\text{SnO}_2$  powder with minor additives (impurity). Due to their excellent energy handling capabilities, they can be applied extensively to protect electronic circuits, various semiconductor devices, and electric power systems from dangerous abnormal transient overload [1, 2].

The first impurity-doped  $\text{SnO}_2$  varistor was reported by Glot and Zlobin [3], and Pianaro et al. also made great contributions to the knowledge of varistor behavior of impurity-doped  $\text{SnO}_2$  ceramics [4]. Through a series of studies on  $\text{SnO}_2$ -based varistors for decades, it is well known that an excellent  $\text{SnO}_2$  varistor system consists of three kinds of dopants: resistance reducers (varistor forming oxide, VFO), densifiers, and modifiers, respectively [5]. To date, the commonly applied VFOs are  $\text{Nb}^{5+}$  [6–8] or  $\text{Ta}^{5+}$  [9–11], which possesses high chemical valence and is soluble in  $\text{SnO}_2$  grains to decrease the grain resistivity; the densifier is insoluble ion of low chemical valence that will segregate at  $\text{SnO}_2$  grain boundary regions to promote the densification by producing oxygen vacancies, for example,  $\text{Co}^{2+}$  [4, 6, 7, 9, 11],  $\text{Mn}^{2+}$

[12, 13], and  $\text{Zn}^{2+}$  [8, 14], and the modifiers can effectively improve the electrical properties of the varistors, such as  $\text{Cr}^{3+}$ ,  $\text{Fe}^{3+}$ ,  $\text{Cu}^{2+}$ , and rare earth elements [6–9, 15, 16].

Moreover, during modern ceramics processing, high energy attrition milling and  $\text{ZrO}_2$  grinding media were often applied. As a result,  $\text{Zr}^{4+}$  contamination in ceramic samples is a common phenomenon. However, up to now, no literature about the role of  $\text{Zr}^{4+}$  ion ( $\text{ZrO}_2$ ) in  $\text{SnO}_2$ -based varistors has been reported.

Recently, we optimized a  $\text{SnO}_2\text{-Ta}_2\text{O}_5\text{-ZnO}$  varistor system, which presents varistors of good nonlinear properties but very low varistor voltage [17]. Based on it, in the present study,  $\text{SnO}_2\text{-Ta}_2\text{O}_5\text{-ZnO}$ -based varistor system was doped with  $\text{ZrO}_2$  (0–2.0 mol%), and the effect of  $\text{ZrO}_2$  doping on the microstructure and nonohmic properties of  $\text{SnO}_2\text{-Ta}_2\text{O}_5$  based varistors was investigated. To our surprise, varistors with fully dense structure and high breakdown voltage could be obtained.

## 2. Experimental Procedure

**2.1. Sample Preparation.** The samples were prepared using a conventional ceramic processing method with a nominal

composition of (99.45- $x$ ) mol% SnO<sub>2</sub> + 0.05 mol% Ta<sub>2</sub>O<sub>5</sub> + 0.5 mol% ZnO +  $x$  mol% ZrO<sub>2</sub> ( $x = 0, 0.25, 0.5, 1.0, 2.0$ ). All the oxides were raw powders of analytical grade. At beginning, the raw powders were mixed in deionized water and ball-milled in polyethylene bottle for 24 h with 0.5 wt% of PVA as binder and highly wear-resistant ZrO<sub>2</sub> balls as grinding media. Subsequently, the obtained slurries were dried at 110°C in an open oven. After drying, the powder chunks were crushed into fine powders, sieved, and pressed into pellets of 6 mm in diameter and 1.5 mm in thickness under a pressure of 40 MPa. Then, the pressed pellets were sintered at 1400°C for 2 h in a Muffle oven by heating at a rate of 300°C/h and cooling naturally. To measure the electrical properties, silver electrodes were prepared on both surfaces of the sintered disks by heat treatment at 500°C for half an hour.

**2.2. Materials Characterization.** The density of the samples was measured by Archimedes method according to international standard (ISO18754). Their crystalline phases were identified by X-ray diffractometer (XRD, D/max2550HB+/PC, Cu K $\alpha$ , and  $\lambda = 1.5418 \text{ \AA}$ ) through a continuous scan mode with speed of 8°/min. The microstructure was examined on the fresh fracture surfaces of the samples via a scanning electron microscope (SEM, Tescan XM5136). And the average size of SnO<sub>2</sub> grains in the samples was determined using linear intercept method from the SEM images.

A high-voltage source measurement unit (Model: CJ1001) was used to record the characteristics of the applied electrical field versus current density ( $E$ - $J$ ) of the samples. The varistor voltage ( $V_B$ ) was determined at 1 mA/cm<sup>2</sup> and the leakage current ( $I_L$ ) was the current density at 0.75 $V_B$ . Then, the nonlinear coefficient ( $\alpha$ ) was obtained by the following equation:

$$\alpha = \frac{\log(J_2/J_1)}{\log(E_2/E_1)} = \frac{1}{\log(E_2/E_1)}, \quad (1)$$

where  $E_1$  and  $E_2$  are the electric fields corresponding to  $J_1 = 1 \text{ mA/cm}^2$  and  $J_2 = 10 \text{ mA/cm}^2$ , respectively.

### 3. Results and Discussion

**3.1. Composition and Microstructure.** Figure 1 illustrates the XRD patterns of the as-prepared SnO<sub>2</sub>-Ta<sub>2</sub>O<sub>5</sub>-ZnO-based varistor ceramics doped with different amounts of ZrO<sub>2</sub>. All the sharp diffraction peaks were assigned, corresponding to the (110), (101), (200), (111), (211), (220), (002), (310), (112), (301), (202), and (321) reflections of SnO<sub>2</sub> cassiterite phase (JCPDS card no. 77-0451). No extra phases were identified, possibly because the doping levels of the additives were too low to be detected in XRD limits. And, because of the same ionic valence and almost no radius difference between Sn<sup>4+</sup> (0.071 nm) and Zr<sup>4+</sup> (0.072 nm) ions, the doped ZrO<sub>2</sub> is fully soluble in SnO<sub>2</sub> lattice, which can be seen from almost the same positions of XRD diffraction peaks of the prepared samples as shown in Figure 1(b) in a close view to the patterns in  $2\theta$  from 50 to 55°. As for the splitting of the XRD peaks in

the figure, it might be due to the peak doublet of K-alpha 1 and K-alpha 2.

SEM images of the as-prepared SnO<sub>2</sub>-Ta<sub>2</sub>O<sub>5</sub>-ZnO based varistor ceramics also confirmed the solubility of ZrO<sub>2</sub> into SnO<sub>2</sub> lattice (please see Figure 2). The images reveal that, although doped with different amounts of ZrO<sub>2</sub>, the typical microstructure of the samples almost has no change: almost fully dense structure of SnO<sub>2</sub> grains without any obvious second phases. The detailed microstructural parameters are also summarized in Table 1. With increasing doping amount of ZrO<sub>2</sub>, the density of samples decreases in a very narrow range from 6.93 to 6.80 g/cm<sup>3</sup> partly because the density of ZrO<sub>2</sub> (5.89 g/cm<sup>3</sup>) is lower than that of the matrix SnO<sub>2</sub> (6.95 g/cm<sup>3</sup>), but the relative density of the samples also decreases although also in a very narrow range from 99.8% to 98.2%, which indicates a decreased sample densification and could be attributed to the lower diffusion ability of solid ZrO<sub>2</sub> particles in SnO<sub>2</sub> matrix at the designed sintering temperature because the melting point of ZrO<sub>2</sub> (2680°C) is much higher than that of SnO<sub>2</sub> (1630°C). Moreover, from these SEM images, it can be clearly seen that, with increasing ZrO<sub>2</sub> contents in the ceramics, the average size of SnO<sub>2</sub> grains decreases, which might be owing to the inhibited transportation of SnO<sub>2</sub> during sintering by the doped ZrO<sub>2</sub> with lower diffusion ability.

**3.2. Electrical Properties.** The  $E$ - $J$  characteristics of the as-prepared SnO<sub>2</sub>-Ta<sub>2</sub>O<sub>5</sub>-ZnO-based ceramic varistors doped with different contents of ZrO<sub>2</sub> are illustrated in Figure 3, and their corresponding detailed electrical parameters calculated from the  $E$ - $J$  curves are listed in Table 1.

The results indicate that, with increasing doping content of ZrO<sub>2</sub> up to 1.0 mol%, the nonlinear coefficient of the samples increased up to 15.9, possibly owing to the increased carrier concentration in the varistors, decreased electrical resistivity of SnO<sub>2</sub> grains and thus enhanced barrier height by doping, and higher number of voltage barriers due to the decrease in grain size, but it would drop down with more ZrO<sub>2</sub> doped, due to the corresponding less dense sample structure, degraded effective grain boundary, destroyed depletion layer structure, and thus decreased barrier height. The leakage current of the samples presented an opposite trend to that of nonlinear coefficient with ZrO<sub>2</sub> doping, and the varistors with 1 mol% ZrO<sub>2</sub> presented the lowest leakage current, 110  $\mu\text{A/cm}^2$ , which is completely consistent with classic theory on their relationship [18]. Thus, it can be concluded that the optimum doping amount of ZrO<sub>2</sub> in the proposed SnO<sub>2</sub>-Ta<sub>2</sub>O<sub>5</sub>-ZnO-based ceramic varistor system was 1 mol%. The varistor voltage of the samples increased monotonously with the doping amount of ZrO<sub>2</sub>, which could be mainly attributed to the decreased SnO<sub>2</sub> grain size, thus increasing the number of grain boundary in unit thickness after doping.

### 4. Conclusions

SnO<sub>2</sub>-Ta<sub>2</sub>O<sub>5</sub>-ZnO varistors doped with different amounts of ZrO<sub>2</sub> (0–2.0 mol%) were prepared by sintering at 1400°C

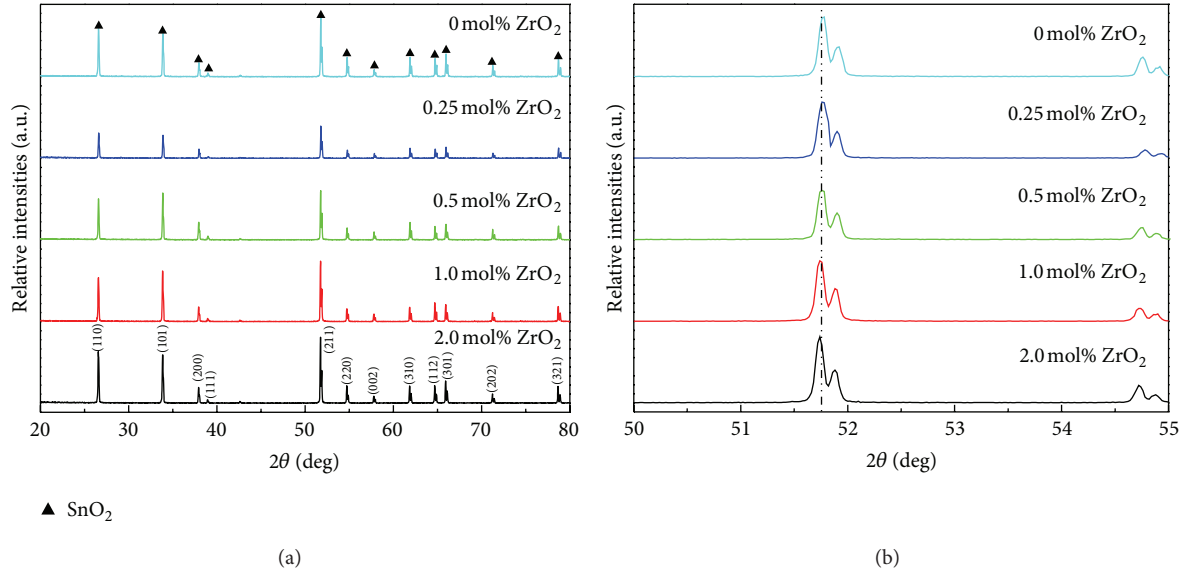


FIGURE 1: XRD patterns of the as-prepared SnO<sub>2</sub>-Ta<sub>2</sub>O<sub>5</sub>-ZnO-based varistor ceramics doped with different amounts of ZrO<sub>2</sub>: (a) five of the samples and (b) magnified view in 2θ region of 50–55°.

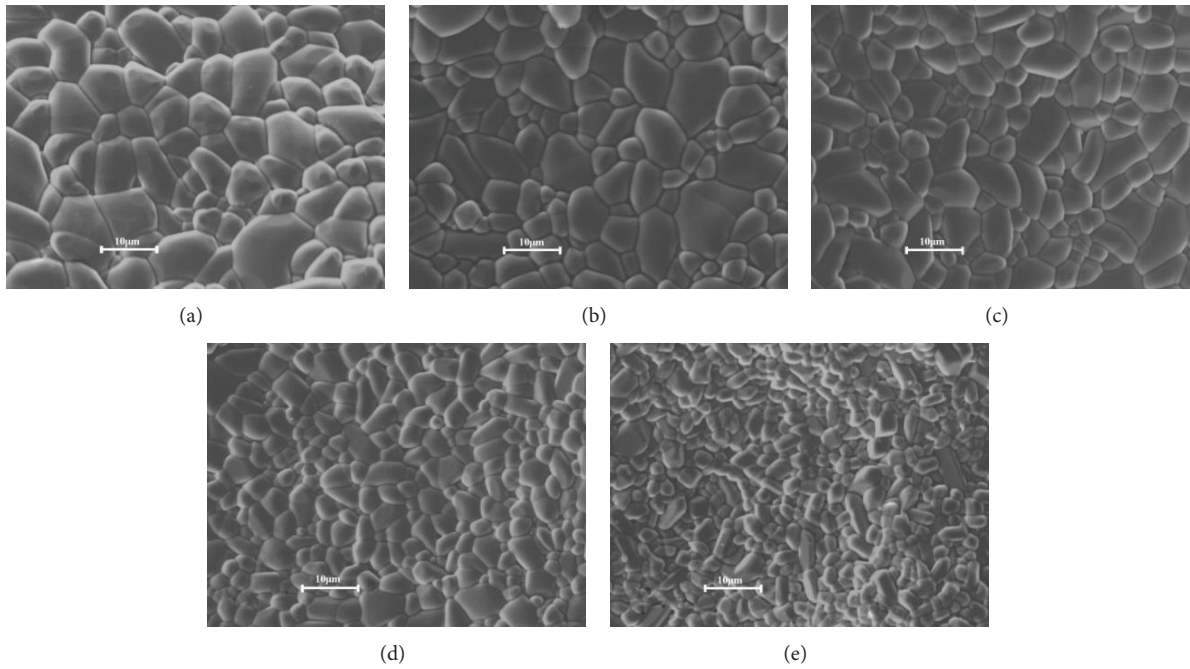


FIGURE 2: Typical SEM images on fracture surfaces of the as-prepared SnO<sub>2</sub>-Ta<sub>2</sub>O<sub>5</sub>-ZnO-based varistor ceramics doped with different amounts of ZrO<sub>2</sub>: (a) undoped, (b) 0.25, (c) 0.5, (d) 1.0, and (e) 2.0 mol%.

TABLE I: Basic physical parameters of SnO<sub>2</sub>-Ta<sub>2</sub>O<sub>5</sub>-ZnO varistor ceramics doped with different contents of ZrO<sub>2</sub>.

Doping amount of ZrO <sub>2</sub> (mol)	Apparent density (g/cm <sup>3</sup> )	Relative density (%)	SnO <sub>2</sub> grain size (µm)	α	V <sub>B</sub> (V/mm)	I <sub>L</sub> (µA/cm <sup>2</sup> )
0	6.93	99.8	7.87	4.6	81	660
0.25	6.89	99.2	6.67	6.0	103	560
0.5	6.88	99.1	5.45	8.2	250	220
1.0	6.84	98.6	4.55	15.9	500	110
2.0	6.80	98.2	3.03	11.6	720	170

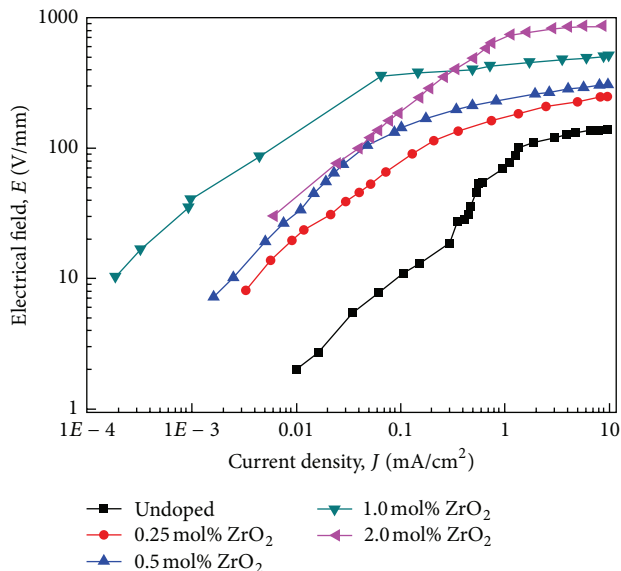


FIGURE 3:  $E$ - $J$  characteristic curves on a log scale at room temperature of the as-prepared  $\text{SnO}_2$ - $\text{Ta}_2\text{O}_5$ - $\text{ZnO}$ -based varistors doped with different contents of  $\text{ZrO}_2$ .

for 2 h with conventional ceramic processing method. The doping of  $\text{ZrO}_2$  would degrade the densification of the varistor ceramics, but inhibit the growth of  $\text{SnO}_2$  grains. In the designed range, varistors with 1.0 mol%  $\text{ZrO}_2$  presented the maximum nonlinear exponent of 15.9 and lowest leakage current of  $110 \mu\text{A}/\text{cm}^2$ ; but the varistor voltage increased monotonously with the doping amount of  $\text{ZrO}_2$ .

## Conflict of Interests

The authors declare that there is no conflict of interests regarding the publication of this paper.

## Acknowledgments

The authors would like to thank the financial support for this work from the National Natural Science Foundation of China (grant nos. 61274015, 11274052 and 51172030), and the Transfer and Industrialization Project of Sci-Tech Achievement (Cooperation Project between University and Factory) from Beijing Municipal Commission of Education.

## References

- [1] P. R. Bueno, J. A. Varela, and E. Longo, "SnO<sub>2</sub>, ZnO and related polycrystalline compound semiconductors: an overview and review on the voltage-dependent resistance (non-ohmic) feature," *Journal of the European Ceramic Society*, vol. 28, no. 3, pp. 505–529, 2008.
- [2] D. R. Leite, M. Cilense, M. O. Orlandi, P. R. Bueno, E. Longo, and J. A. Varela, "The effect of TiO<sub>2</sub> on the microstructural and electrical properties of low voltage varistor based on (Sn,Ti)O<sub>2</sub> ceramics," *Physica Status Solidi A*, vol. 207, no. 2, pp. 457–461, 2010.
- [3] A. B. Glot and A. P. Zlobin, "Non-ohmic conductivity of tin dioxide ceramics," *Inorganic Materials*, vol. 25, pp. 274–276, 1989.
- [4] S. A. Pianaro, P. R. Bueno, E. Longo, and J. A. Varela, "A new SnO<sub>2</sub>-based varistor system," *Journal of Materials Science Letters*, vol. 14, no. 10, pp. 692–694, 1995.
- [5] I. Safaee, M. A. Bahrevar, M. M. Shahraki, S. Baghshahi, and K. Ahmadi, "Microstructural characteristics and grain growth kinetics of Pr<sub>6</sub>O<sub>11</sub> Doped SnO<sub>2</sub>-based varistors," *Solid State Ionics*, vol. 189, no. 1, pp. 13–18, 2011.
- [6] J. F. Wang, W. B. Su, H. C. Chen, W. X. Wang, and G. Z. Zang, "(Pr, Co, Nb)-doped SnO<sub>2</sub> varistor ceramics," *Journal of the American Ceramic Society*, vol. 88, no. 2, pp. 331–334, 2005.
- [7] R. Parra, Y. Maniette, J. A. Varela, and M. S. Castro, "The influence of yttrium on a typical SnO<sub>2</sub> varistor system: microstructural and electrical features," *Materials Chemistry and Physics*, vol. 94, no. 2-3, pp. 347–352, 2005.
- [8] R. Parra, J. A. Varela, C. M. Aldao, and M. S. Castro, "Electrical and microstructural properties of (Zn, Nb, Fe)-doped SnO<sub>2</sub> varistor systems," *Ceramics International*, vol. 31, no. 5, pp. 737–742, 2005.
- [9] J.-F. Wang, H.-C. Chen, W.-B. Su, G.-Z. Zang, B. Wang, and R.-W. Gao, "Effects of Sr on the microstructure and electrical properties of (Co, Ta)-doped SnO<sub>2</sub> varistors," *Journal of Alloys and Compounds*, vol. 413, no. 1-2, pp. 35–39, 2006.
- [10] C.-M. Wang, J.-F. Wang, W.-B. Su, H.-C. Chen, G.-Z. Zang, and P. Qi, "Microstructure development and nonlinear electrical characteristics of the SnO<sub>2</sub>-CuO-Ta<sub>2</sub>O<sub>5</sub> based varistors," *Journal of Materials Science*, vol. 40, no. 24, pp. 6459–6462, 2005.
- [11] G. Zang, J. F. Wang, H. C. Chen et al., "Effects of Sc<sub>2</sub>O<sub>3</sub> on the microstructure and varistor properties of (Co, Ta)-doped SnO<sub>2</sub>," *Journal of Alloys and Compounds*, vol. 377, no. 1-2, pp. 82–84, 2004.
- [12] C. P. Li, J. F. Wang, W. B. Su, H. C. Chen, W. L. Zhong, and P. L. Zhang, "Effect of Mn<sup>2+</sup> on the electrical nonlinearity of (Ni, Nb)-doped SnO<sub>2</sub> varistors," *Ceramics International*, vol. 27, no. 6, pp. 655–659, 2001.
- [13] J. W. Fan, H. J. Zhao, Y. J. Xi, Y. C. Mu, F. Tang, and R. Freer, "Characterisation of SnO<sub>2</sub>-CoO-MnO-Nb<sub>2</sub>O<sub>5</sub> ceramics," *Journal of the European Ceramic Society*, vol. 30, no. 2, pp. 545–548, 2010.
- [14] F. M. Filho, A. Z. Simões, A. Ries, L. Perazolli, E. Longo, and J. A. Varela, "Nonlinear electrical behaviour of the Cr<sub>2</sub>O<sub>3</sub>, ZnO, CoO and Ta<sub>2</sub>O<sub>5</sub>-doped SnO<sub>2</sub> varistors," *Ceramics International*, vol. 32, no. 3, pp. 283–289, 2006.
- [15] H. Bastami, E. Taheri-Nassaj, P. F. Smet, K. Korthout, and D. Poelman, "(Co, Nb, Sm)-doped tin dioxide varistor ceramics sintered using nanopowders prepared by coprecipitation method," *Journal of the American Ceramic Society*, vol. 94, no. 10, pp. 3249–3255, 2011.
- [16] A. V. Gaponov and A. B. Glot, "Electrical properties of SnO<sub>2</sub> based varistor ceramics with CuO addition," *Journal of Materials Science*, vol. 21, no. 4, pp. 331–337, 2010.
- [17] J. F. He, Z. J. Peng, Z. Q. Fu, C. B. Wang, and X. L. Fu, "Effect of ZnO doping on microstructural and electrical properties of SnO<sub>2</sub>-Ta<sub>2</sub>O<sub>5</sub> based varistors," *Journal of Alloys and Compounds*, vol. 528, pp. 79–83, 2012.

- [18] F. Jiang, Z. J. Peng, Y. X. Zang, and X. L. Fu, "Progress on rare-earth doped ZnO-based varistor materials," *Journal of Advanced Ceramics*, vol. 2, no. 3, pp. 201–212, 2013.